THE INTRARENAL DISTRIBUTION
OF TRITIATED PARA-AMINOHIPPURIC ACID
DETERMINED BY A MODIFIED TECHNIQUE
OF SECTION FREEZE-DRY RADIOAUTOGRAPHY

BETRAND BORDIER, LEONARD ORNSTEIN,
and RICHARD P. WEDEEN

From the Departments of Medicine, The Cell Research Laboratory and The Andre Meyer
Department of Physics, Mount Sinai School of Medicine, New York 10029

ABSTRACT

Section freeze-dry radioautography has been used to examine the intrarenal distribution
of a water-soluble organic acid (para-aminohippuric acid (PAH-3H)) under constant-
infusion, steady-state conditions in mouse and rat kidney in vivo. The technique described
here has the following advantages: (a) Sectioning and freeze-drying are accomplished in a
closed cryostat at temperatures below −40°C; (b) Handling of the section is facilitated by
mounting of the section-to-be on adhesive-coated Saran Wrap prior to cutting; (c) Unem-
bedded freeze-dried sections are attached to photographic film at ambient temperature in
the dark room; (d) Fixation follows completion of radioautographic exposure and precedes
photographic development; (e) Permanent close contact is maintained between tissue and
film. Morphologic preservation compared favorably with that obtained by optimal fixation
techniques, which, however, permit diffusion. Cellular accumulation of PAH-3H during
secretion was demonstrated in the proximal tubule under steady-state conditions in vivo.
The cellular concentration of PAH-3H was uniform throughout the length of the proximal
tubule in mouse and rat kidney.

INTRODUCTION

Water-soluble materials can be held in their in vivo
positions by freeze-drying. If freeze-drying is then
followed by radioautography, the intracellular dis-
tribution of water-soluble radioactive materials
can be determined and their concentrations esti-
mated. Previously reported techniques of freeze-
dry radioautography are, however, not entirely
satisfactory (31).

We have improved the technique of freeze-dry
radioautography and have used it to study the
relationship between transepithelial transport and
cellular accumulation of organic acids in the
kidney. We have been able to demonstrate cellular

accumulation of hippuric acid derivatives and
amino acids in the proximal tubules of rat kidney
in vivo (43, 46).

The objective of this paper is to describe recent
modifications of the section freeze-dry radioauto-
graphic method. These modifications result in
improved morphologic quality of tissue, improved
uniformity of the radioautograph, and shortened
exposure times. They eliminate a potential source
of diffusion artifact and facilitate routine staining
of the preparation. Much of the simplicity of the
technique originally described and the ease of
handling freeze-dried sections of varied sizes have

been preserved. Because some of the morphologic distortion in our previous freeze-dried preparations appeared to be due to freezing the relatively large, whole kidney of the rat, we have extended our investigations to the mouse kidney. Using the modified section freeze-dry radioautographic technique, we have demonstrated that tritiated para-aminohippuric acid (PAH-3H) is accumulated relatively homogeneously throughout the length of proximal tubules in mouse, as in rat, under steady-state conditions in vivo.

METHODS

Adult female Swiss white mice, weighing 10–18 g, were fasted overnight but permitted free access to water. The mice were anesthetized by intraperitoneal administration of Inactin, 3 mg, and a tracheotomy tube was inserted. The left jugular vein was cannulated with PE 10 polyethylene tubing, which was then connected to a Harvard infusion pump (Harvard Apparatus Co., Inc., Millis, Mass.).

The infusate consisted of an isotonic sodium bicarbonate solution containing 5–10 mCi of PAH-3H (30–150 μg per ml); inulin, 50 mg per ml; and mannitol, 30 mg per ml. After 120 μl was administered as a priming solution over 2 min, the infusion was delivered at a rate of 3.93 μl per min. The right ureter was ligated via a suprapubic incision, in order to create stop-flow conditions in the right kidney; outflow of urine from the left kidney was unobstructed. The bladder was catheterized with PE 10 tubing, and urine from the left kidney was collected under oil in preweighed microcentrifuge tubes. 60 min after the start of the infusion, urine and blood were collected for a 30 min clearance period.

Immediately after the termination of the infusion, the left ureter and renal pedicle was ligated, and the kidney was promptly excised and immersed in a 2:1 mixture of propane-isopentane precooled to about −170°C in liquid nitrogen. The right kidney was then removed and frozen in a similar fashion. A small lead weight attached to the ligature aided prompt submersion of the kidney in the freezing liquid. The time between ligation of the renal pedicle and completion of freezing was less than 15 sec. Inulin and PAH were measured in urine and plasma by chemical methods (33, 41) or, when PAH-3H was used, by liquid scintillation counting of whole blood (47).

Prior to sectioning, the kidney was removed from the freezing bath in a closed cryostat (Refrigeration for Science, Oceanside, N.Y.) maintained at −65°C. (Specially designed electrically heated gloves [Reflectronic Corp. New York] permit prolonged working periods in the cryostat at temperatures as low as

−86°C). The frozen tissue block was mounted on a precooled chuck with a precooled saturated glucose solution (freezing point, approximately −20°C). The portion of the block above the frozen mounting medium was trimmed down to the plane of interest, and a $\frac{1}{2} \times 1$ inch strip of Saran Wrap coated with heat-cured, low-temperature silicone adhesive (Dow Corning No. 281 [Dow Corning Corp., Midland, Mich.]) was pressed against the face of the frozen tissue block (46). The Saran Wrap serves as a support for the frozen tissue during sectioning. Sections 2μ in thickness were cut with a well sharpened carbon steel microtome knife with a narrow bevel angle of 15°. Sectioning was usually accomplished with a cryostat temperature of −65°C, but no loss of morphologic quality or redistribution of PAH-3H has been noted at working temperatures up to −40°C. To simplify subsequent handling of the Saran-mounted tissue, the Saran Wrap is attached to a $\frac{3}{4} \times 2$ inch strip of 0.002 inch thick Mylar on a microscope slide so that the section faces out. Minimal amounts of the silicone adhesive previously placed on both sides of the Mylar strips hold the Mylar to the glass and the Saran Wrap to the Mylar. Freeze-drying was achieved overnight in a specially designed vacuum chamber in the cryostat at −65°C, as previously described (44). In order to prevent condensation of water on the tissue, the chamber was warmed outside of the cryostat before breaking the vacuum.

In the dark room, the tissue section, backed by Mylar and Saran Wrap, was removed from the glass slide and pressed, tissue down, against a stripping film plate. In order to avoid trapping air, contact must be made between tissue and film before the surrounding adhesive touches the film. The silicone adhesive on the Saran Wrap adheres to the film, helping to maintain good contact and reducing the likelihood of displacement of the section during exposure. The stripping film bearing the tissue and Saran Wrap was stripped from the glass plate and placed with desiccant in a light-tight box at 4°C for radioautographic exposure. When the exposure was completed, the stripping film-tissue-Saran Wrap package was mounted on a precleaned, gelatin-coated microscope slide which had been moistened with a drop of water sufficiently to become tacky. The film was gently pressed against the tacky surface, with section facing up, and allowed to dry for 60 min in air.

Recently we have abandoned use of stripping film in favor of microscope slides precoated with liquid photographic emulsion by the dipping technique (5). The Saran-mounted, freeze-dried section is pressed against the dried emulsion-coated slide. The use of emulsion-coated microscope slides eliminates problems of emulsion swelling, reticulation, and

separation from the slide, which sometimes occurs during processing of the stripping film preparations.

After completion of the radioautographic exposure the silicone adhesive, Mylar and Saran Wrap were removed by soaking the preparation in xylene for 3 hr in the dark. The Saran Wrap drops off in the xylene, leaving the section facing outward (Fig. 1). The forces which keep the tissue section adherent to the film after removal of the adhesive have not been defined. Xylene was removed by two successive 3-min transfers in a semi-anhydrous solution containing acetone, 35% formaldehyde, glacial acetic acid, and water in the proportion of 90:4:1:5, to protect the freeze-dried cell structure against the ravages of later photographic development (7, 11). After transfer to acetone for 3 min and gently running water for 5 min, the film was developed with Kodak D-19 developer for 4 min at 17°C. Development was stopped for 5 min with Kodak nonswelling short stop No. SB-5. The film was then fixed in Kodak general purpose Hardener-Fixer for 5 min, rinsed gently in water for 10 min, and dehydrated in ascending alcohol solutions.

The tissue and underlying developed radioautograph were mounted under mineral oil for phase-contrast and bright field microscopy, or stained by the periodic acid-Schiff (PAS) method as modified by Deimling et al. (8). Nonradioactive control tissue was prepared in a similar fashion in parallel with each batch of experimental tissue.

Luminal and peritubular diameters of tubules cut in cross-section were measured in photomicrographs taken under phase-contrast optics with the aid of a stage micrometer. For the purpose of these measurements the width of the brush border was included in the luminal diameter.

RESULTS

Morphology

Fig. 2 shows the appearance of the subcapsular tubules under free-flow and under stop-flow conditions. Under free-flow conditions, the proximal
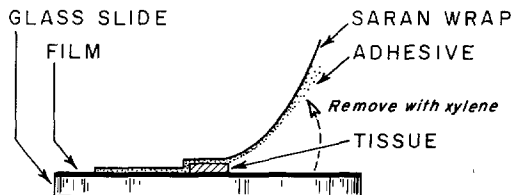

FIGURE 1 Diagrammatic representation of section freeze-dry radioautograph after exposure has been completed and while the Saran Wrap and Dow Corning 281 adhesive are being removed by xylene.

tubules in the outer third of the cortex are collapsed (Fig. 2 a), possibly a consequence of surgically induced outer cortical ischemia (26). After 90 min of stop-flow, the lumina of subcapsular proximal tubules are patent (Fig. 2 b), though less distended than inner cortical nephrons in the same obstructed kidney (Table I and Fig. 3).

The distention of tubules under stop-flow conditions is probably due to back pressure from the occluded urinary collecting system, which maintains luminal patency despite diminished outer cortical blood flow and glomerular filtration. Tubular diameters and calculated tubular wall cross-section areas are presented in Table I. Under stop-flow conditions, the calculated tubular wall cross-section area in the inner cortex is not significantly altered from that in free-flow conditions.

Good morphologic preservation is seen at the cellular level in these section freeze-dry radioautographs. Examination under medium dark phase-contrast illumination with a 100 X oil immersion objective reveals nuclei, mitochondria, and brush borders in proximal tubules (Fig. 3).

The good quality of morphologic preservation can also be seen in stained preparations. In Fig. 4, brush borders and basement membranes have been stained with PAS, and nuclei with hematoxylin. A lightly stained preparation was selected for black and white photomicrography in order not to obscure the radioautograph grains. Brush borders, basement membranes and nuclei are consequently stained just sufficiently to permit identification.

Intrarenal Distribution of PAH-3H

The suitability of the mouse for studies of renal tubular transport of PAH was demonstrated by showing that renal function in this species is comparable to that reported in rat (6). In five studies, plasma PAH clearance averaged 1.48 ml/min per 100 g body weight, and inulin clearance averaged 0.87 ml/min per 100 g body weight (Table II). The filtration fraction averaged 0.57.

Radioautographs demonstrate cellular accumulation of PAH-3H in the proximal tubules of mouse (Figs. 3–5). No cellular accumulation is evident in distal tubules, but radioactivity is present in the lumina of distal tubules (Figs. 3, 4). No definite difference between radioautographs from proximal tubule cells under free-flow and stop-flow kidneys can be discerned by simple inspection.

The over-all PAH-3H distribution pattern in mouse cortex can be seen in the low power photo-
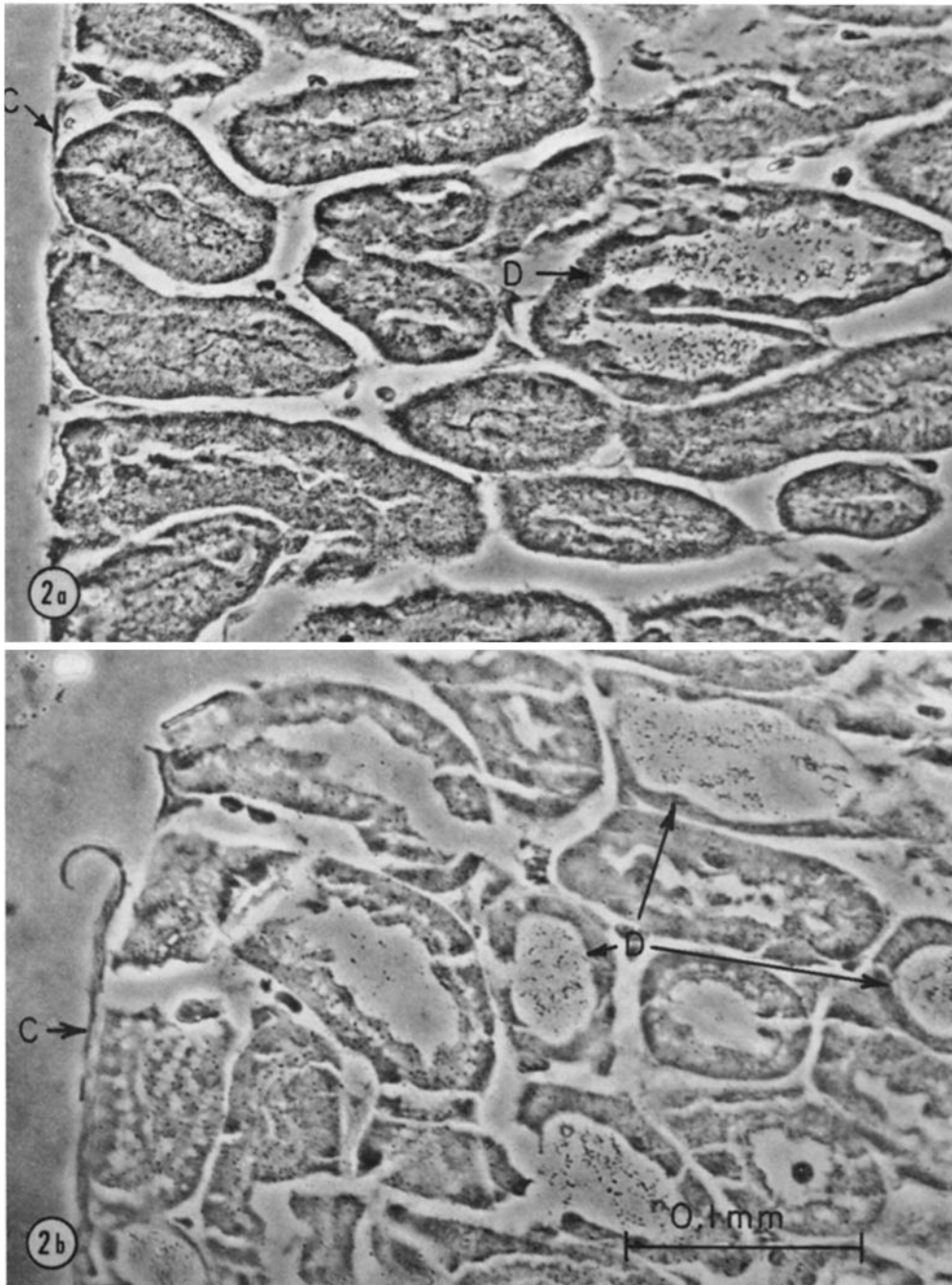
FIGURE 2. Mouse kidney. Phase-contrast photomicrographs of freeze-dried radioautographs. *a*: Outer cortical nephrons from kidney frozen under free-flow conditions. Note collapse of proximal tubule lumina due to cortical ischemia. *b*: Outer cortical nephrons from kidney frozen under stop-flow conditions. *C*, renal capsule; *D*, distal tubule. × 327.

TABLE I

Mouse Tubule Size in Freeze-Dried Sections

Cortex		Luminal diameter*	Peritubular diameter*	Cross-section area of wall*
		μ	μ	μ^2
Free-flow	outer	—	26.3 ± 0.7	—
Free-flow	inner	18.0 ± 1.4	32.0 ± 1.6	551 ± 56
Stop-flow	outer	23.8 ± 1.2	33.8 ± 1.3	455 ± 35
Stop-flow	inner	33.9 ± 1.1	42.4 ± 1.3	508 ± 49

* Mean ± standard error of the mean.

micrograph in Fig. 5. Black regions correspond to luminal radioactivity, predominantly in distal tubules (Fig. 5 b). Between the black areas (high grain density) over the lumina are relatively homogeneous gray areas reflecting cellular accumulation of PAH-3H in all parts of the mouse proximal tubule (Figs. 5 a, b). Since the distal portion of the mouse proximal tubule (including the straight proximal segment) lies close to the medulla (23), it can be seen that there is no increase, and perhaps even a slight decrease, in cellular PAH-3H concentration along the length of the proximal tubule (Figs. 5 a, b).

DISCUSSION

In recent years numerous methods for preparing radioautographs with water-soluble compounds have appeared in the literature. Three approaches have been most extensively explored: (a) Radioautography of frozen sections (1, 14, 38, 48); (b) Radioautography of freeze-dry embedded tissue (12, 35, 43); (c) Section freeze-dry radioautography of unembedded tissue (9, 36, 40, 45). Some of these frozen tissue methods have been carried out at temperatures too high (above −35°C) to assure optimum morphologic preservation and inhibition of diffusion during freezing, sectioning, and drying (1, 9, 12, 14, 38, 40, 48). Application of frozen sections to film (1, 14, 38, 41, 48) in the darkened cryostat presents technical difficulties in handling as well as the possibilities of morphologic change during storage and negative chemography (28). If freeze-dried tissue is embedded before (12, 35) or after (43) sectioning, the labeled material may diffuse into the embedding medium prior to radioautograph exposure. Indeed, the possibility of diffusion is introduced whenever "moisture" (12, 14) or other adhesives (38, 48) are used to attach tissue to photographic film prior to expo-

sure. Most recently, freeze-drying below −40°C has appeared to offer the most generally satisfactory approach to high resolution radioautography of water-soluble substances when fine structure preservation is necessary (38).

Stumpf and Roth (36) have employed a technique of radioautography for diffusible substances which is similar to ours. These workers section and freeze-dry below −60°C and dry-mount the freeze-dried sections on film-coated microscope slides. The method of Stumpf and Roth, however, has several disadvantages. The unsupported frozen sections obtained are usually restricted to about 1 mm in diameter and 1 μ in thickness, and must be removed from the cryostat while frozen for lyophilization. Handling such small unsupported sections in the frozen or freeze-dried state without damaging them presents considerable difficulties. The modified technique described here appears to have all the advantages of the Stumpf and Roth technique, in addition to some that are unique. Our method simplifies section handling by mounting the section-to-be on Saran Wrap prior to cutting. The low-temperature adhesive coating on the Saran Wrap contains no free solvent and does not penetrate the tissue; diffusion at the film surface due to silicone adhesive is therefore not a problem. The silicone adhesive surrounding the section, moreover, helps to maintain good contact between tissue and film during exposure. Although humidity was not controlled in our laboratory, no alteration in PAH distribution could be discerned in relation to seasonal fluctuations in ambient humidity. Morphologic preservation is achieved by fixation of the sections after completion of exposure of the radioautograph. Freeze-drying up to 64 sections simultaneously overnight in the cryostat is possible because of the close proximity between frozen sections and desiccant in the vacuum
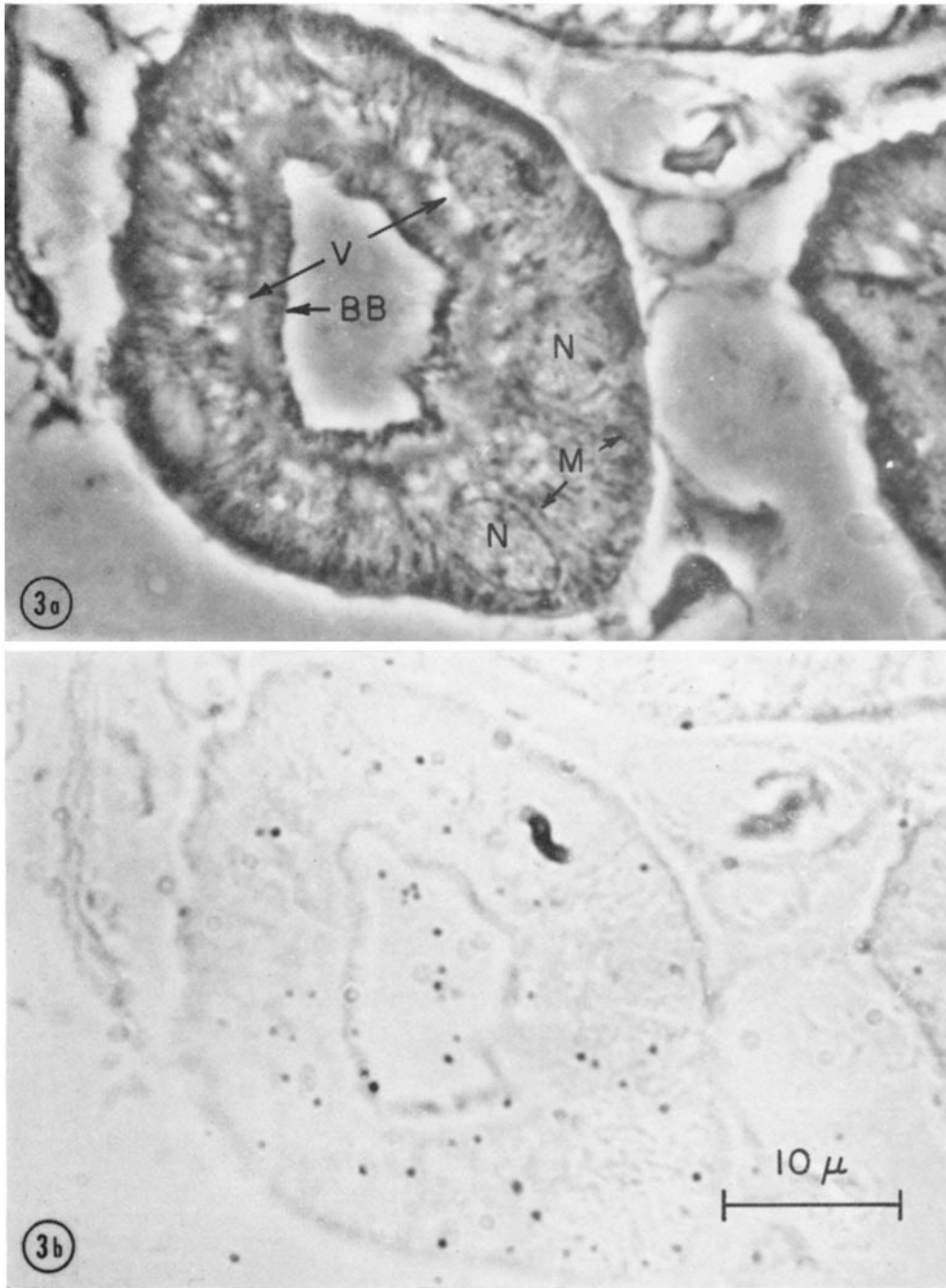
FIGURE 3 Mouse kidney. Phase-contrast image (a) and underlying radioautograph (b). Mitochondria (M), cytoplasmic vacuoles (V), nuclei (N), and brush border (BB) are identifiable in this proximal tubule. This is a patent inner cortical proximal tubule from the same kidney seen in Fig. 2 a. × 2600.
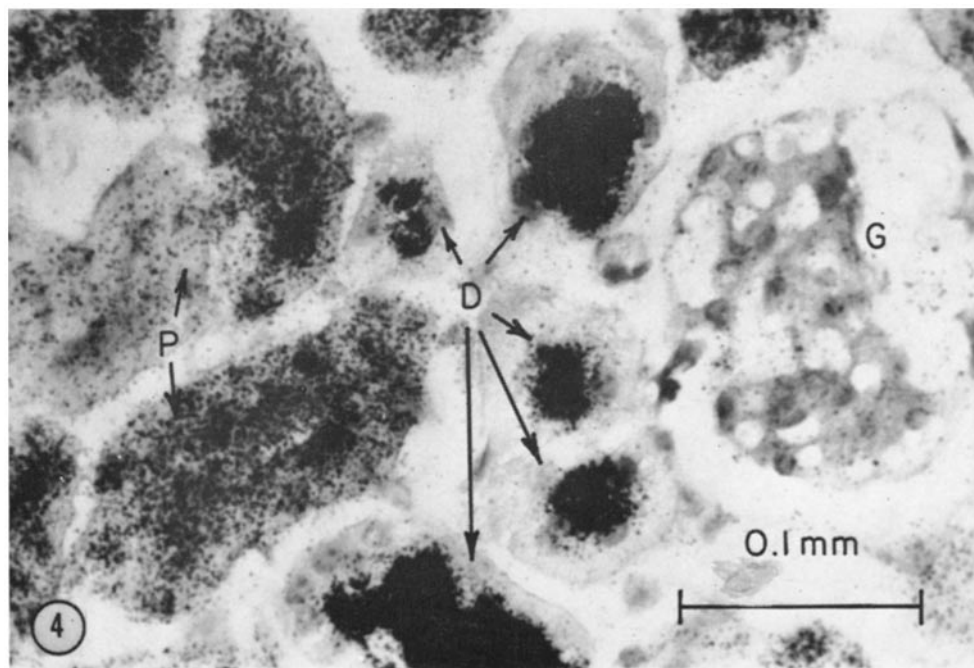
FIGURE 4 Mouse kidney. Lightly stained with PAS and hematoxylin. Radioautograph grains demonstrate cellular accumulation of PAH-3H in proximal tubules (*P*). Highest radioactivity is demonstrated in lumen of distal tubules (*D*). Little radioactivity is demonstrable in glomerulus (*G*). × 327.

TABLE II

Renal Function in Mice

Experiment number	Plasma PAH	PAH clearance	Inulin clearance
		For two kidneys	
	mg%	*ml/min per 100 g body weight*	
1	18.0	2.12	1.46
2	13.2	2.00	.75
3	22.5	1.24	.91
4	9.4	1.12	.51
5	22.5	.94	.72

chamber. Considerable variation in section size is possible.

Previously we used methyl-2-cyanoacrylate (M2C, Eastman 910 [Eastman Chemical Products, Inc., Kings Port, Tenn.]) to attach tissue to film and to embed the tissue section. M2C often prevents even contact between tissue and film; only small areas of good radioautograph contact are therefore obtained. In addition, the probability of diffusion of M2C-soluble substances is introduced. The elimination of M2C simplifies radioautograph preparation, shortens exposure time, and permits routine histologic staining. Image quality is improved by omission of M2C, Saran Wrap, and low-temperature adhesive from the final preparation. Fixation of the sections after radioautograph exposure but prior to development improves the morphologic quality of the tissue sections. In addition, microscope slides precoated with photographic emulsion by "dipping" are easier to handle during developing and staining.

Morphologic preservation in the freeze-dry radioautographs obtained by our method (Fig. 3) is comparable to the best preservation achieved by freeze-drying in other laboratories (2, 10, 16, 22–24, 30), and compares favorably with that obtained by other non-freeze-dry techniques that are designed for optimum structural preservation but permit diffusion (19, 22, 27, 32). Good morphologic preservation requires quick freezing in order to minimize ice-crystal artifact. Because of its smaller size, the whole kidney of the mouse can, of course, be frozen more quickly than that of the rat. Under phase-contrast optics, whole frozen rat kidney (Fig. 8) invariably demonstrates poorer quality than mouse kidney (Fig. 3). If the rat kid-
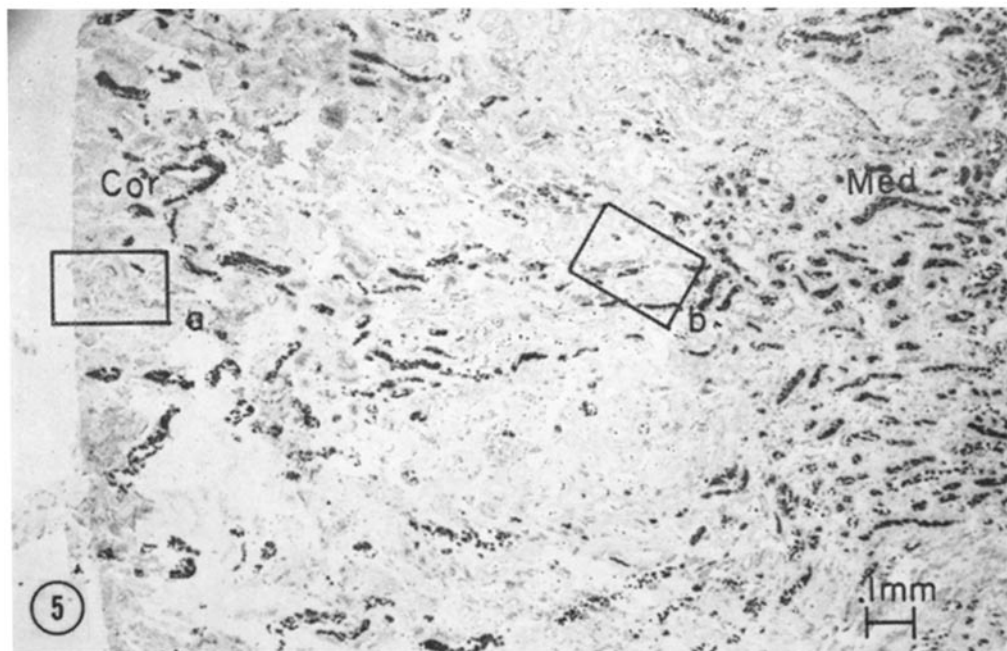
FIGURE 5 Mouse kidney. Radioautograph showing full cortical thickness. Maximum grain density appears over lumen of distal tubules. Faint gray regions represent proximal tubule cell PAH-3H accumulation. No marked gradient in proximal tubule cell concentration of PAH is evident from outer to inner cortex (*Cor*). *Med*, medulla. × 66. Higher magnification of outlined areas from outer cortex (5 *a*) and inner cortex (5 *b*) were photographed with reduced numerical aperture of the condensor in order to show the tissue structures associated with radioautograph grain patterns. × 327.

ney is cut into thin slices (approximately 0.5 mm thickness) prior to freezing (23), a marked improvement in morphologic preservation results. Compare the subcellular morphology of the whole frozen kidney in Fig. 8 to that in the frozen slice radioautograph presented in Fig. 7; nuclei, mitochondria, and brush borders are preserved in the slices (Fig. 7) but are not easily recognizable in the rat kidney frozen whole (Fig. 8). There are some drawbacks, however, to the use of slices in these studies. During slicing, the kidney tubules and blood vessels lose luminal contents, and the tubules collapse. In addition, medium-sized arteries contain no blood that could be used as a convenient internal calibration standard for quantitative radioautography. Also, the trauma and added delay resulting from slicing introduce the possibility of shifts in distribution of substances under study.

Examination of the section freeze-dry radioautographs with the phase-contrast × 100 oil immersion lens demonstrates the quality of the mor-

phologic preservation of kidney tissue at the cellular level (Fig. 3). The quality of morphologic preservation at the tubular level is indicated by comparing the subcortical nephrons in kidneys excised under free-flow and stop-flow conditions (Fig. 2). Luminal diameters under free-flow conditions in our studies are comparable to those found in mice by Hanssen in ischemic mouse kidney cortex (16). The greater luminal diameter found in straight proximal segments compared to convoluted proximal segments, in our studies, is also similar to the findings of Hanssen (16) and Parker (24) in mouse, and Baines and de Rouffignac (3) in rat. As expected, if cell water remains unchanged during ureteral occlusion, inner cortical tubular cell cross-section areas apparently remain constant although both luminal and peritubular diameters increased (Table I). In other words, cell height is approximately inversely proportional to luminal diameter (2). Cell cross-section areas were not measured in collapsed tubules, since it is not usually possible to distinguish brush
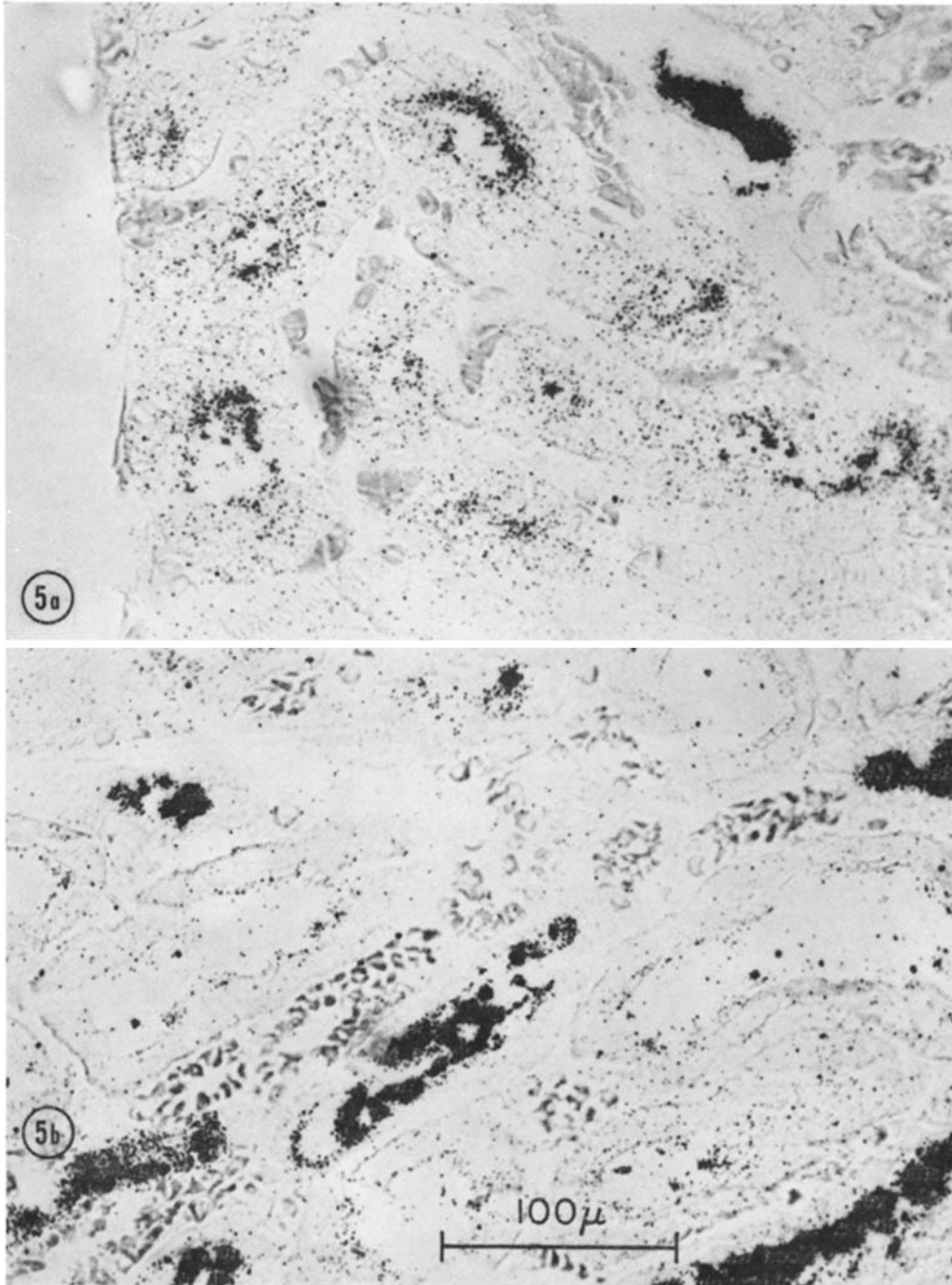
FIGURES 5 a and 5 b   See legend under Fig. 5.

borders from cytoplasm in the phase microscope (4, 15, 18, 20, 21).

Collapse of subcapsular cortical nephrons in these experiments appears to be due to cortical ischemia induced by surgical opening of the abdomen, displacement of viscera, and/or tying of the renal pedicle ligature immediately prior to nephrectomy (13, 26, 42). Subcapsular cortical

luminal collapse is apparently not the result of the histologic precedure, since it can be prevented by stop-flow conditions. Freezing of the whole mouse kidney is begun about 2 sec after nephrectomy, well before luminal collapse, which occurs approximately 20 sec following nephrectomy (2, 16, 18, 20, 24, 34). It therefore seems unlikely that drainage of luminal fluid after interruption of the circulation accounts for tubular collapse in the free-flow kidneys.

These freeze-dry radioautographic preparations are not, however, entirely free of morphologic artifacts. Spaces within cells suggest ice-crystal artifacts. Similarly, large irregular spaces between clumps of silver grains in the radioautographs underlying luminal fluid and urine may, in part, be due to ice-crystal formation and redistribution of dissolved PAH-3H during freezing or drying (Figs. 4, 5 a, 5 b, 7, 8). The relative homogeneity of cellular radioactivity in the proximal tubules may be a consequence of the small size of the ice crystals formed within cells and the presence of a protein matrix upon which the PAH-3H can be distributed as precipitation occurs during freezing or drying. Such protein matrices would be expected in cells, interstitium and blood, but not the urinary spaces. Artifactual spaces due to sectioning can be seen under low magnification (Fig. 2). Major sectioning artifacts, such as fairly regular

parallel breaks in the tubules at right angles to the direction of cutting, are easily recognized.

Some artifactual distortion of interstitial spaces is evident in these preparations as disruption of the tubular basement membranes which usually accompanies preparation of the autoradiographs. In agreement with Leyssac (20), angular distortion of the peritubular surface is most prominent when freezing is delayed (Fig. 7). The intertubular spaces in our freeze-dry preparations are larger than usually seen in post-mortem fixed specimens but appear quite similar to the renal cortical interstitium under conditions designed to avoid changes due to interruption of the circulation (16, 20, 24, 37). The large interstitial spaces observed in quick frozen kidneys apparently reflect the "functional distention of the kidney" in vivo described by Swan (37). To what extent these intertubular spaces may be artifactually enlarged due to continued reabsorption of luminal contents in the short interval between nephrectomy and freezing, as described by Leyssac (19), cannot be determined.

These studies demonstrate proximal tubule cell accumulation of PAH-3H in mouse kidney under steady-state conditions in vivo. The intrarenal distribution pattern of PAH-3H in mouse is similar to that found in rat (Figs. 6–8). While in vivo cellular accumulation of hippuric acid derivatives during transport in rat kidney has been reported
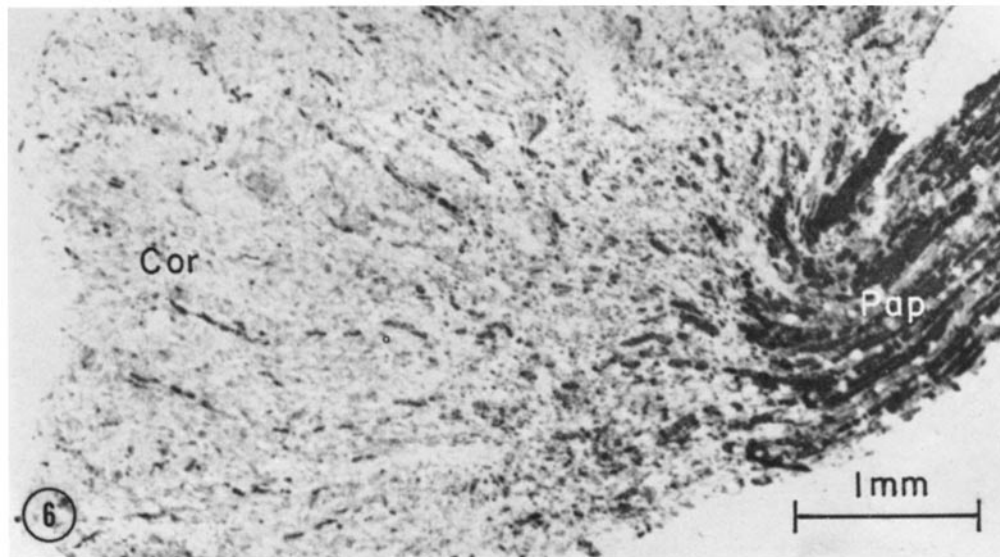

FIGURE 6   Rat kidney. Radioautograph of full kidney thickness. Maximum radioautographic grain density appears over the lumina of distal tubules. No marked progressive increase in cellular PAH concentration can be seen from outer to inner cortex. Cor, cortex; Pap, papilla. × 26.
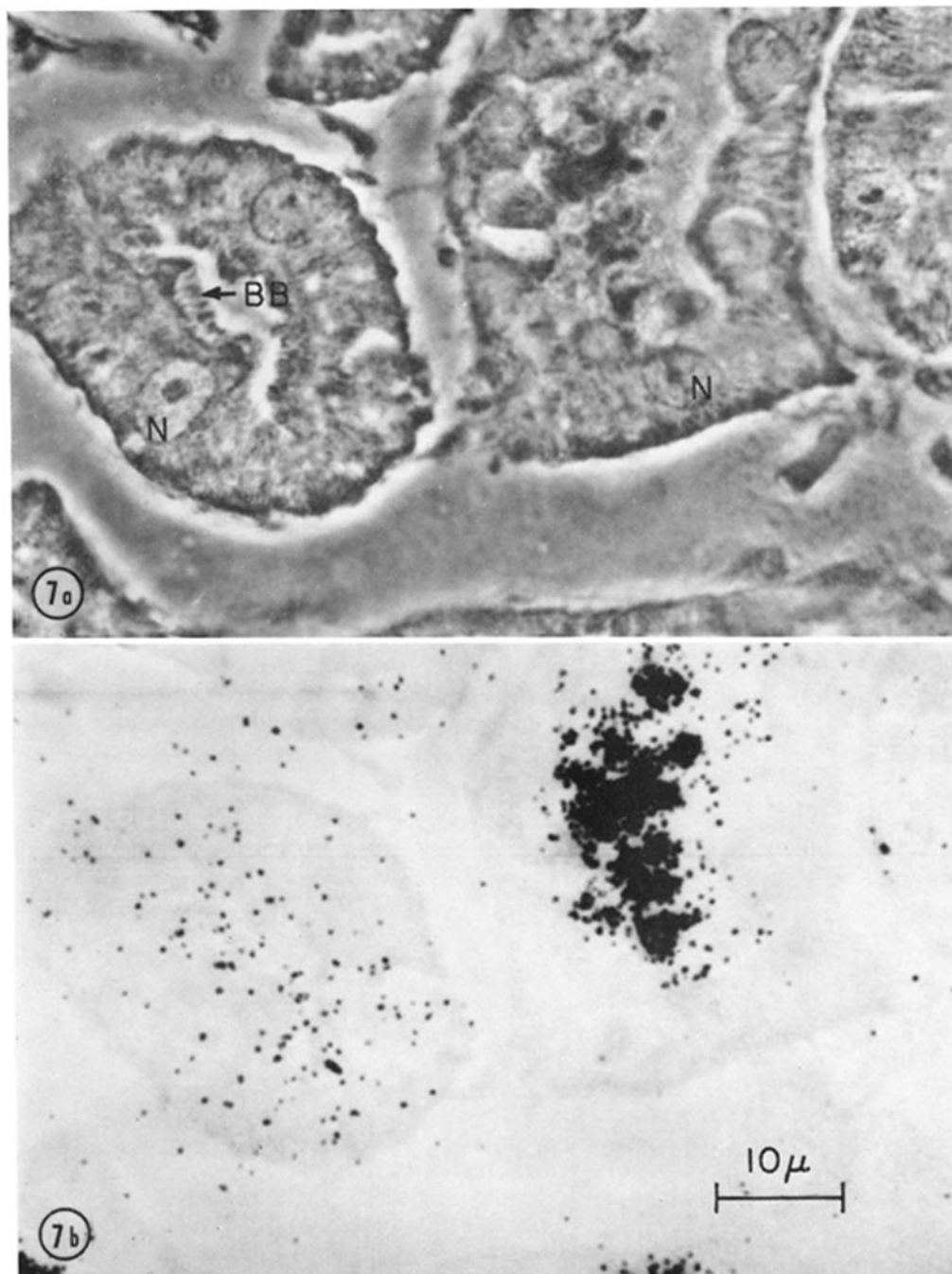
FIGURE 7 Rat kidney. Phase-contrast image (a) and underlying radioautograph (b) showing intrarenal distribution of PAH-3H under steady-state conditions. Kidney frozen after slicing. Radioautograph grains are seen to overlie cells and lumen of proximal tubule and lumen of distal tubule. No grains are seen to overlie distal tubule cells. Proximal tubule lumen collapsed during slicing. Subcellular structure is seen to be well preserved compared to that when whole rat kidney is frozen (Fig. 8). *BB*, brush border; *N*, nucleus. × 1890.
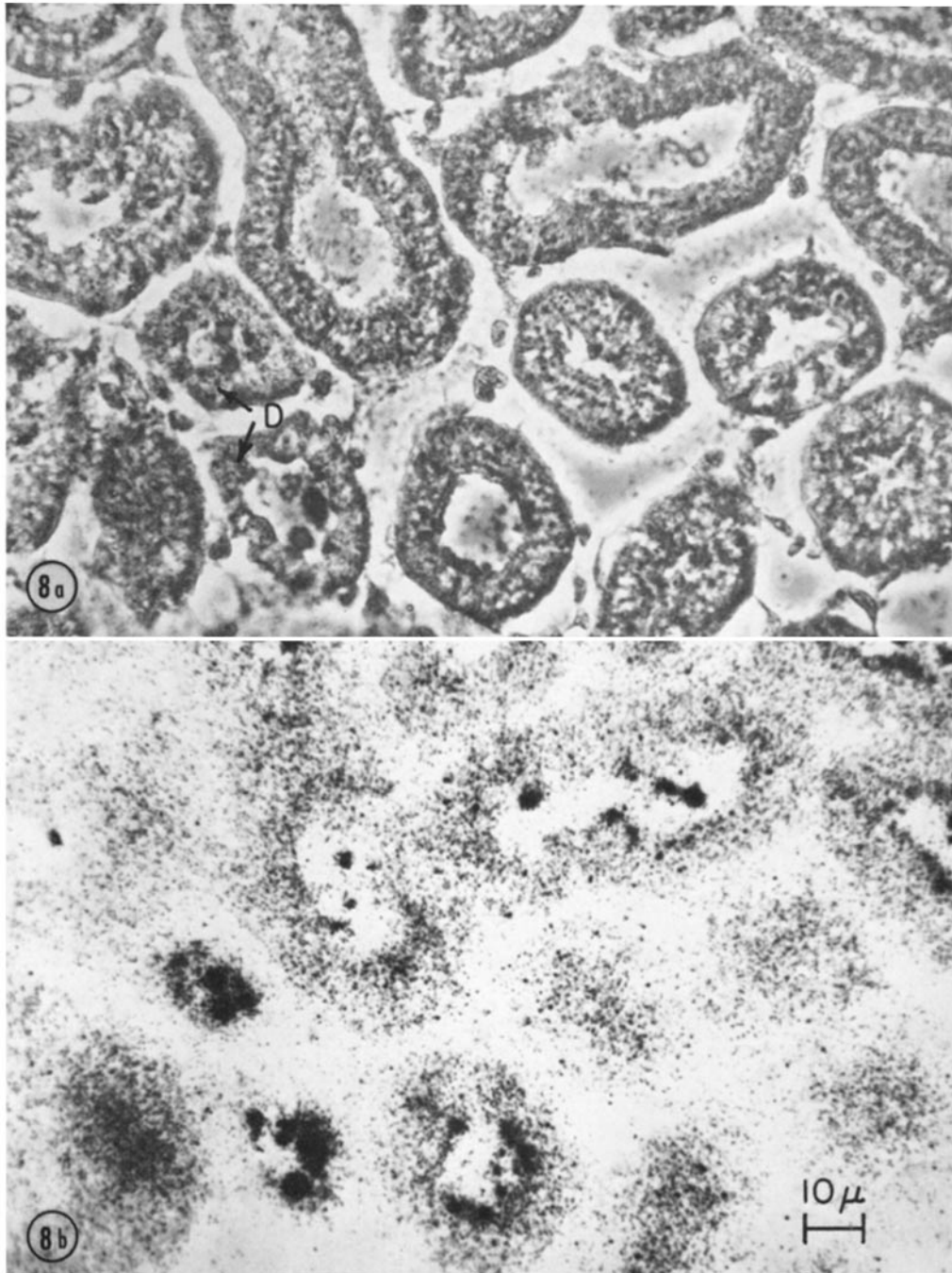
FIGURE 8 Rat kidney. Phase-contrast image (a) and underlying radioautograph (b). Kidney frozen whole. Radioautograph shows accumulation of PAH-3H in cells of proximal tubules but not in distal tubule cells (D). PAH is evident in the lumina of both distal and proximal tubules. Preservation of subcellular structure is poor due to intracellular freezing artifacts. × 800.

previously (43, 46), this is the first demonstration of cellular accumulation of PAH in mouse kidney.

Whether cellular accumulation of PAH is related to transmembrane transport, tubular secretion, tubular reabsorption, or nonspecific intracellular protein binding cannot be determined from these investigations. Some indication of the biologic significance of cellular accumulation of PAH may be gained by comparing the cellular accumulation pattern of PAH with that of other organic acids and by examining the effects of a variety of experimental conditions on the PAH distribution pattern.

Tune, Burg, and Patlak (39) have shown that the isolated perfused rabbit proximal tubule also accumulates PAH intracellularly. However, in their in vitro studies, cells of straight segments of proximal tubules accumulate approximately 20-fold more PAH than do convoluted proximal tubule cells. Increased cellular accumulation in straight proximal tubules compared to convoluted segments has been demonstrated by section freeze-dry radioautography for the nonmetabolized amino acids alpha-aminoisobutyric acid (AIB) and cycloleucine in rat (45). It is clear from our radioautographic studies with PAH-3H that no such marked progressive increase in cell PAH concentration occurs along the length of the proximal tubule under steady-state conditions in the mouse (Fig. 5) or in the rat (Fig. 6) in vivo. A slight increase in cellular PAH concentration in the straight part of the proximal tubule compared to that in the convoluted portion cannot, however, be excluded in rat kidney (Fig. 6) without quantitation of the radioautographs. The explanation of the difference between our findings and those of Tune et al., is not immediately apparent but most likely resides in the facts that they studied a different species and used an in vitro preparation.

Rollhäuser found markedly increased straight proximal segment accumulation of phenol red in rat and rabbit tubules in vivo (29). The intrarenal distribution pattern of phenol red in rabbits is similar to the distribution of the nonmetabolizable amino acids, compounds which are almost completely reabsorbed in the proximal tubule (45). The similarity of intrarenal distribution patterns of the amino acids and phenol red raises the possibility that phenol red is, in fact, partially reabsorbed. Moreover, the observations on phenol red may be subject to artifacts; cellular color induced by phenol red may in part be determined by such unknown factors as intracellular binding and pH.

The modified freeze-dry radioautographic technique described here offers a number of advantages which should make it generally applicable to the study of diffusible compounds in a variety of tissues (17). The quality of morphologic preservation and the uniformity of the radioautographic exposure obtained from mouse kidneys suggest that quantitation by grain counting for estimation of intracellular concentrations of organic acids should be feasible and reasonably reliable with these preparations. In addition, this technique facilitates the handling of freeze-dried sections and therefore should have practical applications in many enzyme-histochemical and immunocytochemical studies as well as in dye and fluorescent physiologic tracer studies (24).

REFERENCES

1. APPLETON, T. C. 1964. Autoradiography of soluble labelled compounds. *J. Roy. Microsc. Soc.* 83:277.

2. BAINES, A. D., C. J. BAINES, and C. DE ROUFFIGNAC. 1969. Functional heterogeneity of nephrons. I. Intraluminal flow velocities. *Pfluegers Arch.* 308:244.

3. BAINES, A. D., and C. DE ROUFFIGNAC. 1969. Functional heterogeneity of nephrons. II. Filtration rates, intraluminal flow velocities and fractional water reabsorption. *Pfluegers Arch.* 308:260.

4. BAINES, A. D., C. W. GOTTSCHALK, and P. P. LEYSSAC. 1968. Proximal luminal volume and fluid reabsorption in the rat kidney. *Acta Physiol. Scand.* 74:440.

5. BELANGER, L. F., and C. P. LEBLOND. 1946. A method for locating radioactive elements in tissue by covering histological sections with photographic emulsion. *Endocrinology.* 39:8.

6. CORTNEY, M. A., M. MYLLE, W. E. LASSITER, and C. W. GOTTSCHALK. 1965. Renal tubular transport of water, solute, and PAH in rats

loaded with isotonic saline. *Amer. J. Physiol.* **209**:1199.

7. DAVIS, B. J., L. ORNSTEIN, P. T. TALEPOROS, and S. KOULISH. 1959. Simultaneous preservation of intracellular morphology and enzymatic or antigenic activities in frozen tissues for high resolution histochemistry. *J. Histochem. Cytochem.* **7**:291.

8. DEIMLING, O. V., K. WITSCH, AND R. ROSSNER. 1968. Methoden zur nachträglichen PAS-und Feulgen-Färbung bei entwickelten autoradiographischen Paraffinschnitten. *Histochemie.* **14**:242.

9. EDELMAN, I. S., R. BOGOROCH, and G. A. PORTER. 1963. On the mechanism of action of aldosterone on sodium transport: The role of protein synthesis. *Proc. Nat. Acad. Sci. U.S.A.* **50**:1169.

10. ECKERT, H. D. 1969. Distribution of soluble substances at the ultrastructural level. *In* Autoradiography of Diffusible Substances. L. J. Roth and W. E. Stumpf, editors. Academic Press Inc., New York. 321.

11. FEDER, N., and R. L. SIDMAN. 1958. Methods and principles of fixation by freeze-substitution. *J. Biophys. Biochem. Cytol.* **4**:593.

12. FITZGERALD, P. J. 1961. "Dry"-mounting autoradiographic technic for intracellular localization of water-soluble compounds in tissue sections. *Lab. Invest.* **10**:846.

13. GOTTSCHALK, C. W., and M. MYLLE. 1956. Micropuncture study of pressures in proximal tubules and peritubular capillaries of the rat kidney and their relation to ureteral and renal venous pressures. *Amer. J. Physiol.* **185**:430.

14. HAMMARSTRÖM, L., L. E. APPELGREN, and S. ULLBERG. 1965. Improved method for light microscopy autoradiography with isotopes in water-soluble form. *Exp. Cell Res.* **37**:608.

15. HANSSEN, O. E. 1960. Early post mortem renal changes studied in mice with one kidney exteriorized. I. The reliability of the experimental method as evaluated by the diuretic response to Mannitol and sodium ferrocyanide. *Acta Pathol. Microbiol. Scand.* **49**:208.

16. HANSSEN, O. E. 1960. Early post mortem renal changes studied in mice with one kidney exteriorized. II. The functional and the early post mortem morphology of the kidney. *Acta Pathol. Microbiol. Scand.* **49**:297.

17. LEHRER, G. M. 1969. The central nervous system sucrose space: A comparison of quantitative and autoradiographic data. *In* Autoradiography of Diffusible Substances. L. J. Roth and W. E. Stumpf, editors. Academic Press Inc., New York, 191.

18. LEYSSAC, P. P. 1963. Dependence of glomerular

filtration rate on proximal tubular reabsorption of salt. *Acta Physiol. Scand.* **58**:236.

19. LEYSSAC, P. P. 1964. The *in vivo* effect of angiotensin on the proximal tubular reabsorption of salt in rat kidneys. *Acta Physiol. Scand.* **62**:436.

20. LEYSSAC, P. P. 1965. Some characteristics of the proximal tubular wall related to reabsorption during luminal occlusion following interruption of glomerular filtration. *Acta Physiol. Scand.* **63**:36.

21. LONGLEY, J. B., and M. S. BURSTONE. 1963. Intraluminal nuclei and other inclusions as agonal artifacts of the renal proximal tubules. *Amer. J. Pathol.* **42**:643.

22. MAUNSBACH, A. B., S. C. MADDEN, AND H. LATTA. 1963. Variations in fine structure of renal tubular epithelium under different conditions of filtration. *J. Ultrastruct. Res.* **6**:511.

23. MAUNSBACH, A. B. 1966. Observations on the segmentation of the proximal tubule in the rat kidney. Comparison of results from phase contrast, fluorescence and electron microscopy. *J. Ultrastruct. Res.* **16**:239.

24. PARKER, M. V., H. G. SWANN, and J. G. SINCLAIR. 1962. The functional morphology of the kidney. *Tex. Rep. Biol. Med.* **20**:425.

25. PEARSE, A. G. E. 1968. Histochemistry: Theoretical and Applied. Third edition. Little Brown & Co. Inc., Boston.

26. POMERANZ, B. H., A. G. BIRTCH, and A. C. BARGER. 1968. Neural control of intrarenal blood flow. *Amer. J. Physiol.* **215**:1067.

27. RHODIN, J. 1958. Anatomy of kidney tubules. *Int. Rev. Cytol.* **7**:485.

28. ROGERS, A. W., and P. N. JOHN. 1969. Latent image stability in autoradiographs of diffusible substances. *In* Autoradiography of Diffusible Substances. L. J. Roth and W. E. Stumpf, editors, Academic Press Inc., New York. 51.

29. ROLLHÄUSER, H. 1957. Histologische und Cytologische Untersuchungen über den Mechanismus der Tubulären Farbstoff Ausscheidung in der Rattenniere. *Z. Zellforschung.* **46**:52.

30. ROTH, L. J. 1969. Autoradiography of diffusible substances. *In* Autoradiography of Diffusible Substances. L. J. Roth and W. E. Stumpf, editors. Academic Press Inc., New York. 1.

31. ROTH, L. J., and W. E. STUMPF, editors. 1969. Autoradiography of Diffusible Substances, Academic Press Inc., New York.

32. ROUILLER, C., and A. F. MILLER, editors. 1969. The Kidney: Morphology, Biochemistry, Physiology, Academic Press Inc., New York. 1.

33. SMITH, W. W., N. FINKELSTEIN, and H. W. SMITH. 1940. Renal excretion of hexitols (sorbitol,

mannitol, and dulcitol) and their derivatives (sorbitan, isomanide, and sorbide) and of endogenous creatinine-like chromogen in dog and man. *J. Biol. Chem.* **135**:231.

34. STEINHAUSEN, M. 1965. Mikrozirkulation von Lissamingrün in der Warmblutniere. Institut für den Wissenschaftlichen Film. **886**:737.

35. STIRLING, C. E., and W. B. KINTER. 1967. High-resolution radioautography of galactose-^{3}H accumulation in rings of hamster intestine. *J. Cell Biol.* **35**:585.

36. STUMPF, W. E., and L. J. ROTH. 1966. High resolution autoradiography with dry mounted freeze-dried frozen sections. Comparative study of six methods using two diffusible compounds ^{3}H-estradiol and ^{3}H mesobilirubinogen. *J. Histochem. Cytochem.* **14**:274.

37. SWANN, H. G. 1960. The functional distension of the kidney. A review. *Tex. Rep. Biol. Med.* **18**:566.

38. TAUGNER, R., H. HOLE, G. GRIGOLEIT, und U. WAGENMANN. 1958. Herstellung geeigneter Gefrierschnitte zur Autoradiographie der Niere in einer Kühlkammer mit eingebautem Mikrotom. *Arch. Exp. Pathol. Pharmakol.* **234**:330.

39. TUNE, B. M., M. B. BURG, and C. S. PATLAK. 1969. Characteristics of p-amino-hippurate transport in proximal renal tubules. *Amer. J. Physiol.* **217**:1057.

40. ULLBERG, S., and L. E. APPELGREN. 1969. Experiences in locating drugs at different levels of resolution. *In* Autoradiography of Diffusible Substances. L. J. Roth and W. E. Stumpf,

editors. Academic Press Inc., New York. 280.

41. VUREK, G. G., and S. E. PEGRAM. 1966. Fluorometric method for the determination of nanogram quantities of inulin. *Anal. Biochem.* **16**:409.

42. WALKER, A. M., and J. OLIVER. 1941. Method for the collection of fluid from single glomeruli and tubules of the mammalian kidney. *Amer. J. Physiol.* **134**:562.

43. WEDEEN, R. P. 1966. Intrarenal localization of C-14-hippuric acid in the rat kidney by autoradiography of freeze-dried sections. III. International Congress of Nephrology—Abstracts.

44. WEDEEN, R. P. 1969. Autoradiography of freeze-dried sections: Studies of concentrative transport in the kidney. *In* Autoradiography of Diffusible Substances. L. J. Roth and W. E. Stumpf, editors. Academic Press Inc., New York. 147.

45. WEDEEN, R. P., S. O. THIER, B. BORDIER, and B. WIENER. 1969. Autoradiographic study of organic acid transport. *Clin. Res.* **27**:453.

46. WEDEEN, R. P., and H. I. JERNOW, 1968. Autoradiographic study of cellular transport of Hippuran-^{125}I in the rat nephron. *Amer. J. Physiol.* **214**:776.

47. WEDEEN, R. P., and B. WEINER. 1969. Extraction of Hippuran-^{131}I and PAH-^{3}H from red blood cells and plasma in the rat. *Amer. J. Physiol.* **217**:838.

48. ZUM WINKEL, K. 1964. Nierendiagnostik mit Radioisotopen. Funktionelle und morphologische Ergebnisse in Experiment und Klinik, Georg Thieme Verlag, Stuttgart.